



HAL
open science

Effect of water warming on the structure of biofilm-dwelling communities

Nabil Majdi, Jana Uthoff, Walter Traunspurger, Pascal Laffaille, Anthony
Maire

► **To cite this version:**

Nabil Majdi, Jana Uthoff, Walter Traunspurger, Pascal Laffaille, Anthony Maire. Effect of water warming on the structure of biofilm-dwelling communities. *Ecological Indicators*, 2020, 117, pp.106622 -. 10.1016/j.ecolind.2020.106622 . hal-03491501

HAL Id: hal-03491501

<https://hal.science/hal-03491501v1>

Submitted on 15 Jul 2022

HAL is a multi-disciplinary open access archive for the deposit and dissemination of scientific research documents, whether they are published or not. The documents may come from teaching and research institutions in France or abroad, or from public or private research centers.

L'archive ouverte pluridisciplinaire **HAL**, est destinée au dépôt et à la diffusion de documents scientifiques de niveau recherche, publiés ou non, émanant des établissements d'enseignement et de recherche français ou étrangers, des laboratoires publics ou privés.



Distributed under a Creative Commons Attribution - NonCommercial 4.0 International License

1 **Effect of water warming on the structure of biofilm-dwelling**
2 **communities**

3 Nabil MAJDI ^{a,b *}, Jana UTHOFF ^a, Walter TRAUNSPURGER ^a, Pascal LAFFAILLE ^b and
4 Anthony MAIRE ^c

5

6 a) *Animal Ecology, Bielefeld University, Bielefeld, Germany.*

7 b) *Laboratoire Ecologie Fonctionnelle et Environnement, EcoLab, Université de Toulouse,*
8 *CNRS, INPT, UPS, Toulouse, France.*

9 c) *EDF R&D LNHE - Laboratoire National d’Hydraulique et Environnement, Chatou,*
10 *France*

11

12 * Corresponding author: N. MAJDI, Email: nabil.majdi@uni-bielefeld.de

13

14

15

16

17

18

19

20

21

22

23

24

25

26 **Abstract**

27 Water warming, either resulting from global or local drivers, is of growing concern for
28 aquatic environments. Changes in thermal regimes may alter the functioning and the trophic
29 dynamics of river ecosystems since most aquatic biota like micro-algae, invertebrates, or fish
30 are poikilotherms. Since biofilms integrate basal and intermediate components of aquatic
31 food webs, examination of their responses to warming should contribute to a better
32 understanding of the effects of ongoing climate change on river ecosystems. In this study, we
33 considered sites that were or were not exposed directly to thermal effluents from a nuclear
34 power plant as “in situ laboratories” of the effect of climate change and water warming. To
35 compare the structure of algal and invertebrate communities dwelling in epilithic biofilms
36 subjected to different thermal regimes in the Garonne River, sets of concrete tiles were placed
37 in the river and the biofilm growing on these standard substrates was sampled after two
38 months of colonisation. The site located within the thermal plume directly downstream of the
39 thermal effluents showed warmer average water temperature (mean ΔT of about 1.5°C over
40 the study period) and greater daily temperature fluctuations in comparison to the control site.
41 Algal and invertebrate biomass did not differ significantly, but the structure of communities
42 differed markedly between sites. At the heated site, the proportion of cyanobacteria was
43 higher, while there were fewer micro-crustaceans and larvae of insects and bivalves.
44 However, the population of chironomids showed a greater proportion of relatively large
45 individuals. Interestingly, nematodes were more abundant, and their communities comprised
46 more species at the heated site. Their feeding-types were also more diverse showing a greater
47 proportion of algivores, large-sized omnivorous and predatory species. Changes in the
48 abundance and age structure further showed that some bacterivore species, such as
49 *Eumonhystera vulgaris*, thrived especially well at the heated site, whereas another
50 bacterivore, *Monhystrella paramacrura*, thrived well at the control site. In the context of

51 climate change, our results highlight that warmer and more fluctuating water temperatures
52 have the potential to alter the body-size spectrum, species composition, distribution of
53 feeding specialisations and age structure within biofilm-dwelling communities.

54

55 **Keywords**

56 Meiofauna, Warming, Freshwater, Community ecology, Species distribution

57 **1. Introduction**

58 The question of how organisms and ecosystems respond to a rise in temperatures has
59 attracted growing attention from the scientific community because of our need to understand
60 and foresee the effects of the ongoing climate change on biological diversity and ecosystem
61 functionality. In aquatic environments, spatial variability in water temperature can be natural
62 (e.g. geothermal activity, presence of a water source) or result from direct local (e.g.
63 deforestation, industrial activities) or indirect global (i.e. climate change) anthropogenic
64 disturbances (Caissie, 2006; Van Vliet et al., 2011). Alteration of thermal regimes can be a
65 major determinant of changes in the diversity and resilience of aquatic biota (Steel et al.,
66 2017; Reid et al., 2019). For example, Mouthon and Daufresne (2006) recorded a dramatic
67 reduction in density and diversity of mollusc communities in the Saône River (France) during
68 the exceptional European heat wave in the summer of 2003. The recovery of the mollusc
69 communities studied was not fully observed even eight years after the heat wave, and
70 profound changes in community structure have persisted over the long term (Mouthon and
71 Daufresne, 2015). Streams and rivers that are naturally or artificially heated can be
72 considered relevant and realistic “*in situ* laboratories” to study the effects of climate change
73 and water warming on aquatic organisms from the individual to the ecosystem level
74 (Woodward et al., 2010). Several examples of such experiments have contributed to a better
75 understanding of the effects of global warming on aquatic biodiversity and ecosystem
76 functioning. In their review, O’Gorman et al. (2012) summarised a decade of research
77 conducted in an active geothermal region (Hengill, Iceland). The underground geothermal
78 heating of streams in this region allowed for comparative studies between naturally heated
79 and non-heated systems. These works have revealed strong influences of water temperature
80 on the structure of macroinvertebrate and algal assemblages, and on ecosystem functioning.
81 Sandblom et al. (2016), Svensson et al. (2017), and Huss et al. (2019) have documented some

82 of the most remarkable results obtained from the “Biotest Enclosure” experiment carried out
83 in the Baltic Sea (Sweden). For research purposes, heated cooling water from a nuclear power
84 plant was diverted into an isolated atoll in the late 1970s. Since then, a temperature difference
85 of 5–10°C has been maintained between the inside and outside of the enclosure. This made
86 possible the study of the physiological responses of the European perch (*Perca fluviatilis*) to
87 water warming, highlighting the fact that global warming could outpace the adaptive capacity
88 of ectotherms (Sandblom et al., 2016). Lastly, Boulêtreau et al. (2014) compared biofilms
89 collected inside or outside the thermal plume of a nuclear power plant located on the Garonne
90 River (France) and demonstrated that water warming affected the denitrification activity of
91 the biofilms through changes in the composition of their bacterial community. Despite the
92 key insights brought by these studies into the responses of aquatic ecosystems to climate
93 change, we still lack a comprehensive understanding of the warming-induced ecological
94 effects that can be expected in the future on more complex and realistic communities made
95 up of different interacting biological compartments.

96 Biofilms are colonies of microscopic organisms that become large enough to create
97 visible, macroscopic structures. In aquatic ecosystems, biofilms are hotspots of biodiversity
98 supporting pivotal ecosystem functions such as primary production and nutrient cycling.
99 Thereby, biofilms fix and transform drifting particles and dissolved inorganic nutrients into
100 attached biomass that can then be used by a variety of consumers (Battin et al., 2016; Lyautey
101 et al., 2013; Risse-Buhl et al., 2012; Romaní et al., 2004; Teissier et al., 2007; Weitere et al.,
102 2018). Ecological successions in river biofilms are characterised by an accretion phase
103 followed by a detachment phase as the thickness and porosity of mature biofilms increase
104 their sensitivity to shear stress and grazers (Biggs, 1996). Nevertheless, biofilms can also
105 self-detach in summer under warmer temperatures and low flow because of bacterial
106 decomposition of senescent basal algal layers (Boulêtreau et al., 2006). The density and

107 biomass of biofilm-dwelling grazers correlate well with the total biomass and chlorophyll *a*
108 content of the biofilm because biofilms represent both a source of food and a habitat for
109 micro-grazers like nematodes (Majdi et al., 2011, 2012a; Peters and Traunspurger, 2005;
110 Schroeder et al., 2012; Vidakovic et al., 2011). Overall, most ecosystem services provided by
111 aquatic biofilms could be strongly affected by global warming (Romaní et al., 2016).
112 Experimental studies of the response of biofilm communities to water warming have shown
113 faster accretion phases (especially higher bacterial growth rates), greater heterotrophic use of
114 organic compounds (Norf et al., 2007; Villanueva et al., 2011), and enhanced filtration rates
115 of peritrich ciliates and rotifers under warmer conditions (Kathol et al., 2009). In a 21-days *in*
116 *situ* warming experiment (on average +2.5°C), warmed-up biofilms showed faster
117 colonisation and maturation, and greater respiration and denitrification rates due to changes
118 in the structure of bacterial communities at the expense of phototrophic biomass (Boulêtreau
119 et al., 2014).

120 The responses of species to water warming essentially depends on their physiological
121 ability to cope with warmer temperatures, or fluctuations thereof, and their capacity to cope
122 with changes in the abundance of the species with which they interact (i.e. their predators,
123 competitors, and prey) (O’Gorman et al., 2012; Woodward et al., 2010). Our aim with this
124 study was to compare heated and non-heated natural river biofilms, with their complex
125 assemblage of prey, micro-grazers, and predators to examine whether their community
126 structure showed coherent responses to different thermal conditions. We exposed biofilms to
127 heated effluents from the nuclear power plant of Golfech (Garonne River, France). At the
128 chosen experimental site, the warming averages +2.5°C (Boulêtreau et al., 2014), which lies
129 in the range of most Earth surface warming scenarios expected for the end of the 21st century
130 (IPCC, 2014). Moreover, the amplitude of daily fluctuating temperatures is increased because
131 of the passage of discharged water in natural draft wet-cooling towers. We monitored the

132 algal and invertebrate communities in biofilms, with particular emphasis on the taxonomic
133 and functional structure of nematodes (numerically dominant metazoans). The biofilms grew
134 during a low-flow period during the summer-fall, right after a substantial heat wave had hit
135 Europe (29 July – 7 August 2018). Our hypotheses regarding the responses of biofilm-
136 dwelling communities to warmer water temperature conditions were: (1) lower algal biomass
137 and changes in the structure of algal communities; (2) changes in the structure of invertebrate
138 communities, especially through the loss of thermosensitive taxa; (3) shift in the size-
139 spectrum of insect larvae due to changes in cohort maturation rates; (4) greater taxonomic
140 and trophic diversity of biofilm-dwelling nematodes, as previously observed in the summer in
141 the Garonne River (Majdi et al., 2011).

142

143 **2. Material and methods**

144 *2.1. Study site*

145 The experiment was conducted from August to October 2018 downstream of the nuclear
146 power plant of Golfech on the Garonne River (SW France, 44°07'04.3"N, 0°50'02.7"E). This
147 nuclear power plant is operated in an open loop with recirculation and is equipped with
148 natural draft wet-cooling towers to reduce the temperature of the blowdown water. The water
149 is withdrawn from the river for its cooling system and the blowdown water is then discharged
150 heated at a series of outlet pipes located directly in the middle of the riverbed over a width of
151 about 100 m (Fig. 1). The resulting thermal plume covers a cone of a few hundred meters
152 long by a hundred meters wide at its base. At this site, the Garonne River is 200 m wide with
153 a relatively shallow (from 0.5 to 1 m depth) riverbed consisting of clayey bedrocks with large
154 stone slabs, cobble bars, or sand/pebbles banks depending on local hydrodynamics, with
155 substantial coverage of several hydrophyte species (e.g., *Potamogeton* spp., *Myriophyllum*
156 *spicatum* L.).

157

158 *2.2. Experimental design*

159 Forty concrete tiles (60 x 40 x 4 cm, 21.5 Kg each) were used as standard substrates for the
160 growth of biofilm and were immersed on 7 August 2018. They were arranged in two blocks
161 of 20 tiles each (5 rows of 4 tiles) facing the flow direction at a depth of 50 cm. One block
162 (heated site) was positioned within the thermal plume, 20 m downstream from the outlet
163 pipes of the nuclear power plant and about 40 m from the right bank of the river (Fig. 1). The
164 other block (control site) was positioned outside the thermal plume on the same transect
165 about 120 m from the right bank of the river (Fig. 1). We observed that each tile in both
166 blocks showed homogeneous and similar depths and bottom flow velocities (depth = 50 ± 2
167 cm; flow velocity = 30 ± 5 cm s⁻¹). A temperature data-logger (measurement frequency = 5
168 min) linked to a buoy was positioned 4 cm above the riverbed and fixed to a steel rod
169 hammered in the riverbed at the centre of each block. Oxygen concentration, conductivity,
170 and pH were recorded monthly using a portable probe (U50, HORIBA) (Table S1 in
171 Appendix). When sampling biofilms, water samples were also collected at each site and
172 analysed after filtration on glass fibre filters (GF/C, Whatman) to measure the concentration
173 of dissolved organic carbon using the combustion catalytic oxidation method (TOC-L,
174 Shimadzu), and of anions and cations using high-performance ionic chromatography (ISC-
175 5000+ and DX-120, Dionex).

176

177 *2.3. Sampling of biofilm*

178 All tiles were sampled on 2 October 2018 (i.e. for a total of 40 samples: one sample per tile
179 with 20 tiles for each of the two sites) after 56 days of immersion; a period deemed long
180 enough to allow for the settlement of mature biofilm communities (Majdi et al., 2012b; Norf
181 et al., 2009). We collected 3.14 cm² patches of biofilm directly underwater using a brush-

182 sampler (Peters et al., 2005). For invertebrates, four patches were collected at random
183 locations on each tile, poured on 20 μ m meshes, and pooled in a 50 ml centrifuge tube.
184 Invertebrate samples were preserved in a buffered formaldehyde solution (final concentration
185 4%) and stained with a few drops Rose Bengal. For algal pigments, two patches were
186 collected and poured in a 50 ml centrifuge tube. Samples were returned to the laboratory in
187 an icebox. The river discharge was very stable (low-flow conditions) during the biofilm
188 colonisation period (i.e. from 7 August to 2 October 2018), but a major flood occurred two
189 weeks after collecting the samples (16 October 2018), which prevented us from continuing
190 the experiment.

191

192 *2.4. Invertebrate identification and data pretreatment*

193 Preserved invertebrates were counted, categorised into size classes (based on maximal length
194 and width), and identified under a dissecting microscope at 40x magnification. While
195 counting, 50 nematode individuals were picked out randomly from each sample,
196 progressively transferred to glycerol, and mounted on slides following the method of
197 Seinhorst (1959). Nematodes were identified at the species level and classified into age and
198 sex categories. Nematode individuals were also classified according to their feeding type
199 based on the morphology of their buccal cavity, after the classification of Traunspurger
200 (1997): deposit-feeders (mainly bacterivorous given the small size of their unarmed buccal
201 cavity), epistrate-feeders (potent algivores given the presence of small teeth in their buccal
202 cavity allowing them to crack diatom frustules), chewers (omnivores or strict predators given
203 their wide mouth armed with large teeth), and suction-feeders (omnivorous or fungal/plant-
204 feeders given that their hollow stylet allows them to perform asymmetrical predation on other
205 animals and hyphae). Thirty individuals of chironomids were also randomly sorted out from
206 each sample during the counting, photographed under the microscope, and measured to the

207 nearest μm using the ImageJ image analysis software. Invertebrate biomass was estimated
208 from allometric relationships found in the literature (see Table S4 in Supplementary
209 Information) and expressed as dry mass per area of biofilm ($\mu\text{gDM } 10\text{cm}^{-2}$).

210

211 *2.5. Pigment analysis*

212 In the laboratory, biofilm samples were pelletized by centrifugation (3000 g, 20 min), freeze-
213 dried, and stored at -80°C until analysis. The pellets were then homogenised and 200 mg
214 subsamples were extracted in 5 mL 98% cold-buffered methanol (with 2% of 1 M ammonium
215 acetate) in a 4°C sonication tub followed by a 15 min extraction in the dark at -20°C . The
216 solution was centrifugated (3000 g, 20 min), the supernatant was kept aside at -20°C , and the
217 pellet was extracted again following the same steps as described above. Thereby, for each
218 sample, a total of 10 mL pigment solution was obtained from which 2 mL was subsampled
219 and filtered through a $0.2 \mu\text{m}$ polytetrafluoroethylene syringe filter. The pigment solution
220 was analysed using a high-performance liquid chromatograph consisting of a 100 mL loop
221 autosampler and a quaternary solvent delivery system coupled to a diode array
222 spectrophotometer (LC1200 series; Agilent). The mobile phase was set after the protocol
223 described by Barlow et al. (1997). Algal pigments were identified and quantified by
224 comparing their retention time and absorption spectra with those of pure standards (DHI LAB
225 products; see Majdi et al., 2011 for further details). We compared the concentration of
226 biomarker pigments typical of specific algal taxonomic groups to estimate potential changes
227 in the composition of the algal community (Jeffrey et al., 1997).

228

229 *2.6. Statistical analyses*

230 All statistical analyses were performed using the ‘vegan’ (Oksanen et al., 2013) and
231 ‘indicpecies’ (Cáceres and Legendre, 2009) packages of the R software (R Development

232 Core Team, 2018). Changes in the pigment composition of the biofilm and the structure of
233 biofilm-dwelling invertebrate and nematode communities between heated and control sites
234 were assessed using permutational analyses of variance based on the Bray-Curtis distance
235 matrices (PERMANOVA, 9999 permutations) calculated from Hellinger-transformed
236 abundance data. Multivariate homogeneity of group dispersion was tested using Anderson's
237 PERMDISP2 procedure which is a multivariate analog of Levene's test and which was met in
238 all cases. We used non-metric multidimensional scaling (nMDS) based on Hellinger-
239 transformed abundance data and Bray-Curtis similarity to ordinate the species in a bi-
240 dimensional space. Sample scores were then plotted as an illustrative variable in this 2D-
241 space to visually assess how different the communities were between the heated and control
242 sites. We used multilevel pattern analysis (9999 permutations) to test the significance of
243 species-site group associations and derive candidate indicator species for each site (Cáceres
244 and Legendre, 2009).

245 We calculated a set of diversity indices based on the untransformed abundances of
246 each taxon in the nematode community. First, the Index of Trophic Diversity (ITD) was
247 computed as $ITD = \sum \theta^2$ with θ being the relative contribution of each of the four functional
248 feeding guilds identified (Heip et al., 1985). This index ranges from 0.25 to 1, which
249 corresponds to the highest (each trophic group contributes 25%) and lowest (only one trophic
250 group present) feeding type diversity, respectively. Species richness (S), Shannon's entropy
251 (H, ln-based), Simpson's dominance (D), and Pielou's evenness (J) were calculated.

252 We used either one-way ANOVA when normality assumptions were met (tested using
253 Shapiro-Wilk and Bartlett test), or non-parametric Kruskal-Wallis rank sum test on
254 untransformed data to test for differences in total abundance and biomass, pigment
255 concentration, diversity indices, the proportion of nematode feeding types, and age ratios
256 between the heated and control sites. Regarding the temperature data and the body mass of

257 chironomid individuals, we compared cumulative density functions between sites using the
258 Kolmogorov-Smirnov test.

259

260 **3. Results**

261 *3.1. Abiotic background*

262 Oxygen, pH, streambed flow velocity, and water depth showed very little variations between
263 sites and along the biofilm colonisation period (Table S1). The most noticeable difference in
264 water chemistry between sites, but minor, was the slightly higher concentrations of major
265 ions like Mg^{2+} , Na^+ , Ca^{2+} , Cl^- , and SO_4^{2-} , which increased water conductivity by 16.3% on
266 average at the heated site (Tables S1 and S2). This difference was probably due to the partial
267 evaporation of the water as it passed through the natural draft wet-cooling towers, thus
268 concentrating the ions in the water discharged upstream of the heated site. Nevertheless, the
269 relative concentration of ions were very similar across sites (Table S2).

270 At the beginning of the colonisation period (7 August 2018), the water temperature
271 was very high ($> 28^{\circ}C$) at both sites (Fig 2A). Water temperature then progressively
272 diminished and the temperature contrast between the control and heated sites became more
273 pronounced in September (Fig. 2C). Overall, the temperature regime differed across the two
274 sites over the 56 days exposure period (total: 1344 h). The control site showed an average
275 temperature of $23.81^{\circ}C$ (min: $19.85^{\circ}C$; max: $28.85^{\circ}C$). The heated site showed an average
276 temperature of $25.32^{\circ}C$ (min: $19.85^{\circ}C$; max: $30.86^{\circ}C$). Thus, the heated site was, on average,
277 $1.5^{\circ}C$ warmer than the control site during the study period (min measured $\Delta T = -2.69^{\circ}C$;
278 max $\Delta T = +4.38^{\circ}C$; Fig. 2C). When comparing the cumulative distribution of temperature
279 functions, there was a significant difference in the local thermal regime between the control
280 and heated sites (Kolmogorov-Smirnov test, $D^+ = 0.47$, $P < 0.001$, Fig. S1). The average daily
281 fluctuation of water temperature (i.e., the range between the minimum and maximum water

282 temperature recorded each day) was also significantly higher at the heated site (on average
283 2.69°C) than at the control site (0.72°C) (Kruskal-Wallis test, $\chi^2 = 90$, $P < 0.001$) (Fig. 2B).

284

285 3.2. Biofilm pigment composition

286 Biofilm pigment composition was significantly different between the heated and control sites
287 (PERMANOVA, $F_{1,38} = 15.8$, $R^2 = 0.29$, $P < 0.001$) (Fig. 3). More specifically, the biofilms
288 showed significantly higher concentrations of chlorophyllide *a*, zeaxanthin, β -carotene,
289 myxoxanthophyll, and echinenone at the heated site in comparison to the control site, while
290 concentrations of chlorophyll *b*, violaxanthin, and lutein were significantly lower at the
291 heated site (Table 1). The concentrations of the most abundant pigments, chlorophyll *a* and
292 fucoxanthin, were not significantly different across sites.

293

294 3.3. Invertebrate community

295 The total abundance of invertebrates was not significantly different across sites (Table 1)
296 with 335.2 ± 38.3 (mean \pm SD) and 295.9 ± 17.3 ind 10cm^{-2} at the control and heated sites,
297 respectively. Nematodes were numerically dominant in the invertebrate community,
298 representing 27.2% and 47.3% of all individuals found at the control and heated sites,
299 respectively (Table 1). The structure of the invertebrate community differed significantly
300 across sites (PERMANOVA, $F_{1,38} = 13.9$, $R^2 = 0.26$, $P < 0.001$) (Fig. 4). Nematodes and
301 oligochaetes were significantly more abundant at the heated site, while larvae of chironomids,
302 *Corbicula*, and Ephemeroptera, as well as harpacticoid copepods and their nauplii larvae,
303 were significantly more abundant at the control site (Table 1). No significant differences in
304 the abundances of rotifers, ostracods, and cladocers were found across sites (Table 1).

305 The estimated total biomass of invertebrates was not significantly different across
306 sites, with 385.8 ± 51.4 (mean \pm SD) and 284.5 ± 58.1 $\mu\text{gDM } 10\text{cm}^{-2}$ at the control and

307 heated sites, respectively (Table 1). Chironomids were strongly dominant in terms of biomass
308 and represented 59.1% and 86.9% of the total invertebrate biomass at the control and heated
309 sites, respectively. The biomasses of Ephemeroptera larvae, *Corbicula* larvae, harpacticoid
310 copepods, ostracods, and nauplii were significantly dampened at the heated site, whereas
311 nematodes showed significantly higher biomass (Table 1). Full test-statistics are provided in
312 Table S3.

313 The individual body-mass of chironomid larvae was on average 5.37 and 9.11 μgDM
314 ind^{-1} at the control and heated sites, respectively (Fig. 5A). Most individuals showed a body-
315 mass $< 1 \mu\text{gDM}$ (Fig. 5A). However, the cumulative distribution function of the chironomid
316 population at the control site was significantly above that of the heated site (Kolmogorov-
317 Smirnov test, $D+ = 0.09$, $P = 0.045$) (Fig. 5B), showing a greater proportion of relatively
318 large chironomid individuals with a body-mass $> 15 \mu\text{gDM}$ at the heated site (Fig. 5B).

319

320 3.4. Nematode community

321 Of the 2,000 nematode individuals that have been identified, a total of 21 species have been
322 found, with 14 and 17 species at the control and heated sites, respectively (Table 2).

323 *Monhystrella paramacrura* (Meyl, 1954), *Eumonhystera vulgaris* (de Man, 1880), and
324 *Chromadorina bioculata* (Schultze in Carus, 1857) were the three dominant species at both
325 sites, accounting cumulatively for approximately 92 and 80% of the total community at the
326 control and heated sites, respectively (Table 2). However, the structure of the nematode
327 community differed significantly across sites (PERMANOVA, $F_{1,38} = 24.8$, $R^2 = 0.39$, $P <$
328 0.001) (Fig. 6). The multilevel pattern analysis highlighted three species that were
329 significantly associated with the heated site (test statistics > 0.56 , $P < 0.008$): the two large
330 predatory-omnivorous *Mylonchulus lacustris* (Cobb, 1915) and *Mesodorylaimus bastiani*
331 (Bütschli, 1873), as well as the bacterivorous *Eumonhystera dispar* (Bastian, 1865).

332 *Mylonchulus lacustris* was absent at the control site while representing approximately 6.3%
333 of the total number of individuals in the community at the heated site. *Mesodorylaimus*
334 *bastiani* was absent at the control site while having a relative abundance of about 5.1% at the
335 heated site. Finally, *E. dispar* was > 10 times more abundant at the heated site (1.71 ind
336 10cm⁻²) in comparison to the control site (0.13 ind 10cm⁻²) (Table 2).

337 Nematode species richness was significantly higher at the heated site (on average 6.95
338 species found in each sample) than at the control site (on average 4.40 species) (Table 1).
339 Shannon's entropy (H) was also significantly higher at the heated site, while Simpson's
340 dominance (D) was lower (Table 1). Pielou's evenness (J) did not differ significantly across
341 sites (Table 1). The index of trophic diversity (ITD) was significantly lower at the heated site,
342 indicating a more homogeneous distribution between the different feeding types (Table 1).
343 Nematode communities were strongly dominated by deposit-feeders at the control site
344 (average relative abundance of 84.2%), while they represented on average only 54.2% of the
345 total abundance at the heated site. In contrast, the relative abundance of epistrate-feeders,
346 chewers, and suction-feeders was significantly higher at the heated site than at the control site
347 (Table 1, Fig. 7).

348 With a substantial number of individuals sampled, we could compare age ratios in the
349 two dominant bacterivorous species, *Monhystrella paramacrura* and *Eumonhystera vulgaris*,
350 across sites. *M. paramacrura* showed a ratio of juveniles:adults significantly lower at the
351 heated site (0.75 and 1.20 at the heated and control sites, respectively; ANOVA, $F_{1,38} = 5.42$,
352 $P = 0.024$). *E. vulgaris* showed a ratio gravid:non-gravid females almost 10x higher at the
353 heated site (0.65 and 0.07 at the heated and control sites, respectively; Kruskal-Wallis, $\chi^2 =$
354 5.3, $P = 0.021$). Other ratios did not differ significantly across sites.

355 **4. Discussion**

356 4.1. A realistic *in situ* warming experiment?

357 Several studies have used naturally or artificially heated streams or river as “*in situ*
358 laboratories” to study the effects of water warming and climate change on aquatic organisms
359 and ecosystem functioning (e.g. Woodward et al., 2010, O’Gorman et al., 2012, Boulêtreau et
360 al., 2014, Worthington et al., 2015, Sandblom et al., 2016). In this study, we carried out an
361 experiment within the thermal plume downstream of heated effluents from a nuclear power
362 plant because we expected that all environmental factors that could influence the structure of
363 the biofilm community (e.g., light, nutrients, hydrodynamics), other than water temperature,
364 would be similar at the two experimental sites (inside or outside the thermal plume). The
365 results on the abiotic environment showed that, given our caution regarding local
366 hydrodynamics, this hypothesis was verified, and thus water temperature appeared to be the
367 major environmental determinant that differed between the heated and control sites. During
368 the experiment, the average difference in water temperature between the control and heated
369 sites was about 1.5°C, which is within the range of optimistic projections of temperature
370 increases by the end of the century (IPCC, 2014). The passage through natural draft wet-
371 cooling towers implies a partial evaporation of the cooling water, thus concentrating
372 dissolved substances in the released effluent. We observed this effect also for dissolved
373 nutrients like nitrate and phosphate. However, when comparing their relative concentrations,
374 we found minor differences between sites, suggesting that the nutrient balance was similar for
375 biofilm-dwelling organisms at both sites. For example, the nitrate:phosphate ratio was 42.5
376 and 41.9 at the control and heated sites, respectively. The passage of the water through
377 natural draft wet-cooling towers, whose efficiency primarily varies with air humidity, has
378 also resulted in greater daily fluctuations in water temperature. Those secondary effects
379 probably enhanced the environmental contrast found across sites. Nevertheless, they also are
380 compatible with future climate change scenarios as the frequency of heat waves are expected

381 to increase in line with the rise in temperature and evaporation (Michel et al., 2019; Morrill et
382 al., 2005; Webb, 1996). It is worth noting that the experimental heated site was located within
383 the thermal plume only 20 m downstream from the outlet pipes of the nuclear power plant.
384 This area does not correspond to the regulatory downstream area (which is located a few
385 kilometres further downstream, after complete mixing between the river and the cooling
386 water released) where ecological differences potentially induced by the operation of the
387 nuclear power plant are under regulatory control, in accordance with local legislation and the
388 requirements of the Water Framework Directive.

389

390 *4.2. Effects of water warming on the microphytobenthic community of biofilms*

391 At both sites, we found relatively high concentrations of fucoxanthin and diadinoxanthin,
392 which are two biomarker pigments for diatoms. This result is consistent with previous studies
393 that have highlighted that epilithic biofilms of the Garonne River were strongly dominated by
394 diatoms in terms of biomass (Boulêtreau et al., 2014; Majdi et al., 2011, 2012a; Tekwani et
395 al., 2013). However, the absence of significant differences in fucoxanthin and diadinoxanthin
396 concentrations across sites showed that diatom biomass was not affected by the temperature
397 contrast studied. Similarly, chlorophyll *a* concentration (as a proxy of phototrophic biomass)
398 did not vary significantly across sites. However we found that the concentrations of
399 chlorophyllide *a*, myxoxanthophyll, and echinenone were more than twice as high at the
400 heated site in comparison to the control site. These three latter pigments are reported
401 biomarkers for cyanobacteria (Hertzberg et al., 1971; Hodgson et al., 2004; Takaichi and
402 Mochimaru, 2007). Several studies showed that warming can selectively promote
403 cyanobacterial growth in rivers (Butterwick et al., 2005; Watkinson et al., 2005). Majdi et al.
404 (2011, 2012a) and Tekwani et al. (2013) also reported an increase of the relative biomass of
405 cyanobacteria in the plankton and in biofilms of the Garonne River during summer low-flow

406 periods. Further studies should focus on identifying which species of cyanobacteria are
407 favoured under warmer conditions and how such changes in the structure of the
408 microphytobenthic community could affect biofilm grazers and the ecosystem-level functions
409 supported by biofilm communities.

410

411 *4.3. Effects of water warming on invertebrate communities*

412 We found that the total abundance of invertebrates did not differ across sites. However, the
413 structure of the community was different, with a relatively diverse community at the control
414 site whereas, at the heated site, it was crowded with nematodes and oligochaetes but lacked
415 micro-crustaceans, larvae of *Corbicula*, and Ephemeroptera. Given the standard procedures
416 used to sample biofilm and the relatively straightforward changes observed at coarse
417 taxonomic-level, our results point out a potential to indicate water warming effects based on
418 changes in the taxonomic structure of biofilm-dwelling invertebrates. It is possible that the
419 warmer temperature and/or the greater daily fluctuation of temperature could have negatively
420 affected thermosensitive taxa such as Ephemeroptera, which need time to acclimatise to
421 critically high temperatures (Houghton and Shoup, 2014). For *Corbicula* larvae, Weitere et
422 al. (2009) showed that a 3°C increase in water temperature could reduce body-mass,
423 reproduction rate, and increase mortality. Such a rise in temperature occurred almost daily at
424 the heated site during the experimental period. In contrast, biofilm-dwelling nematodes and,
425 in a lesser extent, oligochaetes thrived well at the heated site. In addition to warmer average
426 temperatures, greater thermal fluctuations may also represent a stress for aquatic biota
427 (Coulter et al., 2016; Thome et al., 2016), which could lead to the selection of species able to
428 cope with temperature extremes and large temperature fluctuations.

429 In our study, chironomids were the major contributors to invertebrate biomass.

430 However, the reduction of their abundance observed at the heated site did not result in a

431 reduction in total invertebrate biomass. We further showed that this was due to the presence
432 of chironomid individuals that were, on average, twice as large at the heated site in
433 comparison to the control site. Ectotherms can develop adaptive responses to warming such
434 as increased investment in reproduction, decreased body-size at sexual maturity, or higher
435 heat tolerance limits (Daufresne et al., 2009; Loisel et al., 2019; Majdi et al., 2019; Nelson et
436 al., 2017; Ohlberger, 2013; Sandblom et al., 2016; Yvon-Durocher et al., 2011). We did not
437 observe such a reduction of the size spectrum for chironomids. The potential rationales to this
438 result are probably complex and must take into account the fact that (1) we have no
439 information at the species-level for chironomids, therefore we cannot rule out the hypothesis
440 that different species assemblages at the heated site may account for the observed body-size
441 differences. (2) Chironomids complete only part of their life cycle in the aquatic
442 environment. For larvae destined to metamorphose and leave the aquatic environment,
443 warmer temperatures have the potential to boost larval growth and reduce the duration of the
444 larval stage, thereby hastening cohort succession (Cheney et al., 2019). The increase in the
445 size of chironomids observed in our study could therefore also result from the hastening of
446 early summer cohorts. Temperature-boosted larvae could also emerge earlier, with potential
447 far-ranging consequences for species' ecology and biogeography. Nevertheless, this is likely
448 context- and time-dependent. Further large-scale studies examining chironomid communities
449 at a finer taxonomic-level are needed before envisaging the development of a bio-indicator of
450 river warming based on the shape of the size spectrum of chironomids (but see Walker et al.,
451 1991 for bio-indication of past climate based on fossil chironomid species assemblages
452 preserved in lake sediments).

453

454 *4.4. Changes in the structure of nematode communities*

455 We observed that the structure of nematode communities differed across sites, both in terms
456 of species composition and in terms of feeding-type composition. There is evidence that the
457 taxonomic and feeding-type structure of freshwater nematode assemblages can shift in
458 response to broad-scale mechanisms like ecosystem productivity and disturbance regime
459 (Barbuto and Zullini, 2005; Kazemi-Dinan et al., 2014; Majdi et al., 2011; Michiels and
460 Traunspurger, 2005; Ristau et al., 2013; Höss et al., 2011). Here we observed that nematode
461 diversity was greater at the heated site, and we identified a few species that were clearly
462 associated with heated biofilms: *Mylonchulus lacustris*, *Mesodorylaimus bastiani* and
463 *Eumonhystera dispar*. The latter is a rather small opportunistic species, thus it made sense to
464 find it at the heated site. However, the former two species are relatively large and it was
465 surprising that they thrived well at the heated site. Whether those species can be considered
466 indicators of thermal effects in river biofilms needs further studies. However, it has to be
467 noted that several freshwater nematode species have been already classified as sensitive or
468 tolerant to toxic pollution in freshwater sediments leading to the development of a “nematode
469 species at risk” index (NEMAspear; Höss et al., 2011). Among the most common species
470 dwelling river sediments, Höss et al. (2011) showed that *Eumonhystera dispar* was also one
471 of the most resistant to metal and organic pollutions.

472 Warming can affect biomass production and food web structure with mixed effects,
473 from body size-reductions and shortening of food chains in laboratory microbial food webs
474 (Petchey et al., 1999), to body-size increases and elongation of food chains in natural
475 geothermal streams (Woodward et al., 2016). For nematodes, we observed that the
476 distribution between the different feeding-types was more even at the heated site than at the
477 control site. The community was also made up of a greater number of large-sized omnivorous
478 or predatory species at the heated site. In addition, *Chromadorina bioculata*, an algivorous
479 species typical of epilithic biofilms of the Garonne River (Majdi et al. 2011), was about five

480 times more abundant at the heated site than at the control site. These results suggest that
481 warming fostered the establishment of an assemblage of nematodes with more diverse
482 feeding-types, which would presumably play a more important role in trophic transfers in
483 comparison with the control site. Previous studies examining the biofilm ecological
484 succession in the Garonne River have shown that warmer temperatures during summer low-
485 flow periods can trigger profound change in the structure of the algal and bacterial
486 communities (Leflaive et al., 2008; Lyautey et al., 2005; Tekwani et al., 2013) with
487 consequences on nutrient cycling and standing stocks available for grazers (Boulêtreau et al.,
488 2014; Graba et al., 2014; Teissier et al., 2007). Free-living nematodes show complex trophic
489 behaviours including feeding-selectivity and attraction to food patches (Derycke et al., 2016;
490 Estifanos et al., 2013; Höckelmann et al., 2004; Moens et al., 2013; Schroeder et al., 2010).
491 Although more studies are needed to establish robust causalities, we may presume that the
492 presence of a more functionally diverse assemblage of nematode species could be explained
493 by at least two mechanisms: (1) A diversification of food resources that nematodes could
494 exploit in the biofilm, hence agreeing with studies showing the importance of bottom-up
495 effects at structuring nematode communities (Michiels and Traunspurger, 2005; Ristau et al.,
496 2013). (2) Predation and/ or competition for resources as several studies have shown that
497 many organisms can prey on or compete with freshwater nematodes (Majdi and
498 Traunspurger, 2015). A decrease in competition for biofilm basal resources (due e.g. to the
499 reduction of Ephemeroptera and *Corbicula* larvae) may have increased the number of trophic
500 niches available for algivorous nematodes. Furthermore, the decrease in intraguild
501 competition between omnivores and predators (as the numbers of micro-crustaceans and
502 insect larvae were dampened at the heated site) may have favoured the establishment of
503 relatively large omnivorous and predatory nematode species instead. Nematodes are
504 extremely abundant in biofilms and their feeding type does not require specific taxonomic

505 expertise to be recognized under the microscope. Previous studies have shown that the
506 distribution of feeding types within freshwater nematode communities can be influenced by
507 key environmental drivers such as ecosystem productivity (see Traunspurger et al., 2020, and
508 references therein). Whether nematode feeding types may be envisaged as a straightforward
509 indicator of disturbance needs further confirmation, but this is promising as we showed a
510 more even distribution of feeding types at the heated site.

511 Not all nematode species thrived well in warmed-up biofilms. The case of
512 *Monhystrella paramacrura* was especially striking. Although this species was commonly
513 found at both sites, the abundance of this species was half as low at the heated site as at the
514 control site. This difference was accompanied by a much lower number of juveniles in
515 comparison to the control site. This result suggests that populations of *M. paramacrura* were
516 seemingly less successful under a warmer and more fluctuating temperature regime. This
517 response may be physiological as free-living nematodes show species-specific thermal niches
518 with associated patterns of population growth rate, age structure, egg production, or body-
519 size at maturity (Majdi et al., 2019). An average temperature difference of 1.5°C across
520 experimental sites did not seem huge at first. However, Majdi et al. (2019) have evidenced
521 the existence of temperature thresholds between 25 and 30°C above which survival and
522 population growth rate of several freshwater nematode species could be severely reduced.
523 Such upper temperature tolerance thresholds were more likely to be exceeded at the heated
524 site due to an overall higher temperature and a greater amplitude of daily temperature
525 fluctuations. Over the whole 1344 h of study, water temperatures were >25°C for 229 h (i.e.
526 17% of time) and 814 h (i.e. 61%) at the control and heated sites, respectively. This likely
527 explains the reduced success of *M. paramacrura*, at the heated site. Furthermore, nematodes
528 can associate a certain temperature with conditions of food availability and thereby exhibit
529 active attraction or repulsion to a given temperature where appropriate (Mohri et al., 2005).

530 *M. paramacrura* is a small species with a very slender body and a minute mouth cavity
531 without teeth. This may constrain the diet of *M. paramacrura*. On the other hand,
532 *Eumonhystera vulgaris* belongs to the same feeding guild as *M. paramacrura*, but unlike *M.*
533 *paramacrura*, *E. vulgaris* was very successful at the heated site showing higher abundances
534 and a much greater number of gravid females. In comparison, to *M. paramacrura*, *E. vulgaris*
535 is a bit larger showing a larger mouth cavity. Thereby, its diet could have been less limited by
536 prey size, which might be advantageous in warmed-up biofilms. Indeed, at this stage, it is
537 premature to suggest what precisely causes such a species turnover, laboratory studies
538 examining the effects of different conditions of food and temperature on single species and
539 species mixtures could help identify underlying mechanisms more accurately.

540

541 **5. Conclusion**

542 The studied differences in thermal regime did not affect neither the biomass of biofilm-
543 dwelling phototrophs nor the total abundance and biomass of invertebrates. However, the
544 community structure was different with a higher proportion of cyanobacteria and nematodes
545 and lower abundances of crustaceans and insects under warmer conditions. The response of
546 the dominant invertebrate groups in terms of biomass (chironomids) and abundance
547 (nematodes) was further examined, and the results suggested that the body-size structure of
548 chironomids and the taxonomic and functional structure of nematode assemblages could be
549 good tools to indicate the impact of warming on river biofilm communities. The highlighted
550 differences in body-size and community structure may be explained by direct modification of
551 the metabolism and different specific tolerances to temperatures among biofilm-dwelling
552 organisms. The shifted biofilm landscape may, in return, create conditions that are beneficial
553 (or not) for the further settlement of colonists. In summary, our results suggest that water
554 warming coupled with larger daily temperature fluctuations have the potential to profoundly

555 affect biofilm communities. Further studies are recommended to correlate those community
556 shifts to potential changes in important ecosystem functions supported by river biofilms.

557

558 **6. Acknowledgements**

559 We are grateful to Sylvain Lamothe, Louna Riem, Stephanie Boulêtreau, and Arthur Compin
560 for their help in the field and Stefanie Gehner for mounting the nematodes prior to their
561 identification. We also thank the PAPC platform (UMR EcoLab) and Frederic Julien and
562 Didier Lambrigot for their help with water analyses and HPLC. We thank Électricité de
563 France for their financial support and for providing part of the data. We thank two
564 anonymous reviewers for their helpful comments on a previous version of the manuscript.
565 We thank Helena Adão and our meiobenthologist colleagues for invigorating discussions and
566 hosting the 17th International Meiofauna Conference in Evora in July 2019, which has
567 resulted in the preparation of this special issue “Meiofauna in a changing world”.

568

569 **7. References**

- 570 Barbuto, M., Zullini, A., 2005. The nematode community of two Italian rivers (Taro and
571 Ticino). *Nematology* 7, 667–675.
- 572 Barlow, R.G., Cummings, D.G., Gibb, S.W., 1997. Improved resolution of mono- and divinyl
573 chlorophylls a and b and zeaxanthin and lutein in phytoplankton extracts using
574 reverse phase C-8 HPLC. *Marine Ecology Progress Series* 161, 303–307.
- 575 Battin, T.J., Besemer, K., Bengtsson, M.M., 2016. The ecology and biogeochemistry of
576 stream biofilms. *Nature Reviews Microbiology* 14, 251.
- 577 Biggs, B.J.F., 1996. Patterns in benthic algae of streams, in: Stevenson R. J, Bothwell M. L,
578 Lowe R. L (Eds.), *Algal Ecology: Freshwater Benthic Ecosystems*. Academic Press,
579 San Diego, CA, USA, pp. 31–56.

580 Boulêtreau, S., Garabetian, F., Sauvage, S., Sanchez-Perez, J.M., 2006. Assessing the
581 importance of a self-generated detachment process in river biofilm models.
582 *Freshwater Biology* 51, 901–912.

583 Boulêtreau, S., Lyautey, E., Dubois, S., Compin, A., Delattre, C., Touron-Bodilis, A.,
584 Mastrorillo, S., Garabetian, F., 2014. Warming-induced changes in denitrifier
585 community structure modulate the ability of phototrophic river biofilms to denitrify.
586 *Science of the Total Environment* 466, 856–863.

587 Butterwick, C., Heaney, S.I., Talling, J.F., 2005. Diversity in the influence of temperature on
588 the growth rates of freshwater algae, and its ecological relevance. *Freshwater*
589 *Biology* 50, 291–300.

590 Cáceres, M.D., Legendre, P., 2009. Associations between species and groups of sites: indices
591 and statistical inference. *Ecology* 90, 3566–3574.

592 Caissie, D., 2006. The thermal regime of rivers: a review. *Freshwater Biology* 51, 1389–
593 1406.

594 Cheney, K.N., Roy, A.H., Smith, R.F., Dewalt, R.E., 2019. Effects of Stream Temperature
595 and Substrate Type on Emergence Patterns of Plecoptera and Trichoptera From
596 Northeastern United States Headwater Streams. *Environmental Entomology* 48,
597 1349–1359.

598 Coulter, D.P., Sepúlveda, M.S., Troy, C.D., Höök, T.O., 2016. Species-specific effects of
599 subdaily temperature fluctuations on consumption, growth and stress responses in
600 two physiologically similar fish species. *Ecology of Freshwater fish* 25, 465–475.

601 Daufresne, M., Lengfellner, K., Sommer, U., 2009. Global warming benefits the small in
602 aquatic ecosystems. *Proceedings of the National Academy of Sciences* 106, 12788–
603 12793.

604 Derycke, S., De Meester, N., Rigaux, A., Creer, S., Bik, H., Thomas, W.K., Moens, T., 2016.

605 Coexisting cryptic species of the *Litoditis marina* complex (Nematoda) show
606 differential resource use and have distinct microbiomes with high intraspecific
607 variability. *Molecular Ecology* 25, 2093–2110.

608 Estifanos, T.K., Traunspurger, W., Peters, L., 2013. Selective feeding in nematodes: a stable
609 isotope analysis of bacteria and algae as food sources for free-living nematodes.
610 *Nematology* 15, 1–13.

611 Graba, M., Sauvage, S., Majdi, N., Mialet, B., Moulin, F.Y., Urrea, G., Buffan-Dubau, E.,
612 Tackx, M., Sabater, S., Sanchez-Pérez, J.-M., 2014. Modelling epilithic biofilms
613 combining hydrodynamics, invertebrate grazing and algal traits. *Freshwater Biology*
614 59, 1213–1228.

615 Heip, C., Vincx, M., Vranken, G., 1985. The ecology of marine nematodes. Aberdeen
616 University Press.

617 Hertzberg, S., Liaaen-Jensen, S. t, Siegelman, H.W., 1971. The carotenoids of blue-green
618 algae. *Phytochemistry* 10, 3121–3127.

619 Höckelmann, C., Moens, T., Jüttner, F., 2004. Odor compounds from cyanobacterial biofilms
620 acting as attractants and repellents for free-living nematodes. *Limnology and*
621 *Oceanography* 49, 1809–1819.

622 Hodgson, D.A., Vyverman, W., Verleyen, E., Sabbe, K., Leavitt, P.R., Taton, A., Squier,
623 A.H., Keely, B.J., 2004. Environmental factors influencing the pigment composition
624 of in situ benthic microbial communities in east Antarctic lakes. *Aquatic Microbial*
625 *Ecology* 37, 247–263.

626 Houghton, D.C., Shoup, L., 2014. Seasonal changes in the critical thermal maxima of four
627 species of aquatic insects (Ephemeroptera, Trichoptera). *Environmental Entomology*
628 43, 1059–1066.

629 Höss, S., Claus, E., Von der Ohe, P.C., Brinke, M., Güde, H., Heininger, P., Traunspurger,

630 W., 2011. Nematode species at risk — A metric to assess pollution in soft sediments
631 of freshwaters. *Environment International* 37, 940–949.

632 Huss, M., Lindmark, M., Jacobson, P., van Dorst, R.M., Gårdmark, A., 2019. Experimental
633 evidence of gradual size-dependent shifts in body size and growth of fish in
634 response to warming. *Global change biology*.

635 IPCC, 2014. *Climate Change 2014: Synthesis Report. Contribution of Working Groups I, II*
636 *and III to the Fifth Assessment Report of the Intergovernmental Panel on Climate*
637 *Change*. IPCC.

638 Jeffrey, S.W., Mantoura, R.F.C., Wright, S.W., 1997. *Phytoplankton pigments in*
639 *oceanography: guidelines to modern methods*. UNESCO publishing, Paris, France.

640 Kathol, M., Norf, H., Arndt, H., Weitere, M., 2009. Effects of temperature increase on the
641 grazing of planktonic bacteria by biofilm-dwelling consumers. *Aquatic Microbial*
642 *Ecology* 55, 65–79.

643 Kazemi-Dinan, A., Schroeder, F., Peters, L., Majdi, N., Traunspurger, W., 2014. The effect
644 of trophic state and depth on periphytic nematode communities in lakes.
645 *Limnologica* 44, 49–57.

646 Leflaive, J., Boulêtreau, S., Buffan-Dubau, E., Ten-Hage, L., 2008. Temporal patterns in
647 epilithic biofilm-relation with a putative allelopathic activity. *Fundamental and*
648 *Applied Limnology* 173, 121–134.

649 Loisel, A., Isla, A., Daufresne, M., 2019. Variation of thermal plasticity in growth and
650 reproduction patterns: Importance of ancestral and developmental temperatures.
651 *Journal of Thermal Biology* 84, 460–468.

652 Lyautey, E., Hallin, S., Teissier, S., Iribar, A., Compin, A., Philippot, L., Garabetian, F.,
653 2013. Abundance, activity and structure of denitrifier communities in phototrophic
654 river biofilms (River Garonne, France). *Hydrobiologia* 716, 177–187.

655 Lyautey, E., Jackson, C.R., Cayrou, J., Rols, J.-L., Garabétian, F., 2005. Bacterial
656 Community Succession in Natural River Biofilm Assemblages. *Microbial Ecology*
657 50, 589–601.

658 Majdi, N., Mialet, B., Boyer, S., Tackx, M., Leflaive, J., Boulêtreau, S., Ten-Hage, L., Julien,
659 F., Fernandez, R., Buffan-Dubau, E., 2012a. The relationship between epilithic
660 biofilm stability and its associated meiofauna under two patterns of flood
661 disturbance. *Freshwater Science* 31, 38–50.

662 Majdi, N., Tackx, M., Buffan-Dubau, E., 2012b. Trophic positioning and microphytobenthic
663 carbon uptake of biofilm-dwelling meiofauna in a temperate river. *Freshwater*
664 *Biology* 57, 1180–1190.

665 Majdi, N., Traunspurger, W., 2015. Free-living nematodes in the freshwater food web: a
666 review. *Journal of Nematology* 47, 28–44.

667 Majdi, N., Traunspurger, W., Boyer, S., Mialet, B., Tackx, M., Fernandez, R., Gehner, S.,
668 Ten-Hage, L., Buffan-Dubau, E., 2011. Response of biofilm-dwelling nematodes to
669 habitat changes in the Garonne River, France: influence of hydrodynamics and
670 microalgal availability. *Hydrobiologia* 673, 229–244.

671 Majdi, N., Traunspurger, W., Fueser, H., Gansfort, B., Laffaille, P., Maire, A., 2019. Effects
672 of a broad range of experimental temperatures on the population growth and body-
673 size of five species of free-living nematodes. *Journal of Thermal Biology* 80, 21–36.

674 Michel, A., Brauchli, T., Lehning, M., Schaepli, B., Huwald, H., 2019. Stream temperature
675 evolution in Switzerland over the last 50 years. *Hydrology and Earth System*
676 *Sciences*.

677 Michiels, I.C., Traunspurger, W., 2005. Impact of resource availability on species
678 composition and diversity in freshwater nematodes. *Oecologia* 142, 98–103.

679 Moens, T., Vafeiadou, A.-M., De Geyter, E., Vanormelingen, P., Sabbe, K., De Troch, M.,

680 2013. Diatom feeding across trophic guilds in tidal flat nematodes, and the
681 importance of diatom cell size. *Journal of Sea Research* 92, 125–133.

682 Mohri, A., Kodama, E., Kimura, K.D., Koike, M., Mizuno, T., Mori, I., 2005. Genetic control
683 of temperature preference in the nematode *Caenorhabditis elegans*. *Genetics* 169,
684 1437–1450.

685 Morrill, J.C., Bales, R.C., Conklin, M.H., 2005. Estimating stream temperature from air
686 temperature: implications for future water quality. *Journal of Environmental*
687 *Engineering* 131, 139–146.

688 Mouthon, J., Daufresne, M., 2015. Resilience of mollusc communities of the River Saone
689 (eastern France) and its two main tributaries after the 2003 heatwave. *Freshwater*
690 *Biology* 60, 2571–2583.

691 Mouthon, J., Daufresne, M., 2006. Effects of the 2003 heatwave and climatic warming on
692 mollusc communities of the Saône: a large lowland river and of its two main
693 tributaries (France). *Global Change Biology* 12, 441–449.

694 Nelson, D., Benstead, J.P., Huryn, A.D., Cross, W.F., Hood, J.M., Johnson, P.W., Junker,
695 J.R., Gíslason, G.M., Ólafsson, J.S., 2017. Shifts in community size structure drive
696 temperature invariance of secondary production in a stream-warming experiment.
697 *Ecology* 98, 1797–1806.

698 Norf, H., Arndt, H., Weitere, M., 2009. Responses of biofilm-dwelling ciliate communities to
699 planktonic and benthic resource enrichment. *Microbial Ecology* 57, 687–700.

700 Norf, H., Arndt, H., Weitere, M., 2007. Impact of local temperature increase on the early
701 development of biofilm-associated ciliate communities. *Oecologia* 151, 341–350.

702 O’Gorman, E.J., Pichler, D.E., Adams, G., Benstead, J.P., Cohen, H., Craig, N., Cross, W.F.,
703 Demars, B.O., Friberg, N., Gíslason, G.M., 2012. Impacts of warming on the
704 structure and functioning of aquatic communities: individual-to ecosystem-level

705 responses, in: *Advances in Ecological Research*. Elsevier, pp. 81–176.

706 Ohlberger, J., 2013. Climate warming and ectotherm body size—from individual physiology
707 to community ecology. *Functional Ecology* 27, 991–1001.

708 Oksanen, J., Blanchet, F.G., Kindt, R., Legendre, P., Minchin, P.R., O’hara, R.B., Simpson,
709 G.L., Solymos, P., Stevens, M.H.H., Wagner, H., 2013. Package ‘vegan.’
710 Community ecology package, version 2.

711 Petchey, O.L., McPhearson, P.T., Casey, T.M., Morin, P.J., 1999. Environmental warming
712 alters food-web structure and ecosystem function. *Nature* 402, 69.

713 Peters, L., Scheifhacken, N., Kahlert, M., Rothhaupt, K.O., 2005. Note: An efficient in situ
714 method for sampling periphyton in lakes and streams. *Archiv für Hydrobiologie* 163,
715 133–141.

716 Peters, L., Traunspurger, W., 2005. Species distribution of free-living nematodes and other
717 meiofauna in littoral periphyton communities of lakes. *Nematology* 7, 267–280.

718 R Development Core Team, 2018. R: A language and environment for statistical computing.
719 R Foundation for Statistical Computing. Retrieved from <http://R-project.org>, Vienna,
720 Austria.

721 Reid, A.J., Carlson, A.K., Creed, I.F., Eliason, E.J., Gell, P.A., Johnson, P.T.J., Kidd, K.A.,
722 MacCormack, T.J., Olden, J.D., Ormerod, S.J., Smol, J.P., Taylor, W.W., Tockner,
723 K., Vermaire, J.C., Dudgeon, D., Cooke, S.J., 2019. Emerging threats and persistent
724 conservation challenges for freshwater biodiversity. *Biological Reviews* 94, 849–873.

725 Risse-Buhl, U., Trefzger, N., Seifert, A.-G., Schönborn, W., Gleixner, G., Küsel, K., 2012.
726 Tracking the autochthonous carbon transfer in stream biofilm food webs. *FEMS*
727 *Microbiology Ecology* 79, 118–131.

728 Ristau, K., Faupel, M., Traunspurger, W., 2013. Effects of nutrient enrichment on the trophic
729 structure and species composition of freshwater nematodes—a microcosm study.

730 Freshwater Science 32, 155–168.

731 Romaní, A.M., Boulêtreau, S., Diaz Villanueva, V., Garabetian, F., Marxen, J., Norf, H.,
732 Weitere, M., 2016. Microbes in aquatic biofilms under the effect of changing
733 climate, in: *Climate Change and Microbial Ecology: Current Research and Future*
734 *Trends*. Caister Academic Press, Norfolk, UK, pp. 83–96.

735 Romaní, A.M., Guasch, H., Munoz, I., Ruana, J., Vilalta, E., Schwartz, T., Emtiazi, F.,
736 Sabater, S., 2004. Biofilm structure and function and possible implications for
737 riverine DOC dynamics. *Microbial Ecology* 47, 316–328.

738 Sandblom, E., Clark, T.D., Gräns, A., Ekström, A., Brijs, J., Sundström, L.F., Odelström, A.,
739 Adill, A., Aho, T., Jutfelt, F., 2016. Physiological constraints to climate warming in
740 fish follow principles of plastic floors and concrete ceilings. *Nature Communications*
741 7, 11447.

742 Schroeder, F., Muschiol, D., Traunspurger, W., 2010. Fluctuating food availability may
743 permit coexistence in bacterivorous nematodes. *Fundamental and Applied*
744 *Limnology* 178, 59–66.

745 Schroeder, F., Traunspurger, W., Pettersson, K., Peters, L., 2012. Temporal changes in
746 periphytic meiofauna in lakes of different trophic states. *Journal of Limnology* 71,
747 216–227.

748 Seinhorst, J.W., 1959. A rapid method for the transfer of nematodes from fixative to
749 anhydrous glycerin. *Nematologica* 4, 67–69.

750 Steel, E.A., Beechie, T.J., Torgersen, C.E., Fullerton, A.H., 2017. Envisioning, quantifying,
751 and managing thermal regimes on river networks. *BioScience* 67, 506–522.

752 Svensson, F., Karlsson, E., Gårdmark, A., Olsson, J., Adill, A., Zie, J., Snoeijs, P., Eklöf, J.S.,
753 2017. In situ warming strengthens trophic cascades in a coastal food web. *Oikos*
754 126, 1150–1161.

755 Takaichi, S., Mochimaru, M., 2007. Carotenoids and carotenogenesis in cyanobacteria:
756 unique ketocarotenoids and carotenoid glycosides. *Cellular and Molecular Life*
757 *Sciences* 64, 2607.

758 Teissier, S., Torre, M., Delmas, F., Garabetian, F., 2007. Detailing biogeochemical N budgets
759 in riverine epilithic biofilms. *Journal of the North American Benthological Society*
760 26, 178–190.

761 Tekwani, N., Majdi N, Mialet B, Tornés E, Urrea-Clos G, Buffan-Dubau E, Sabater S, Tackx
762 M, 2013. Contribution of epilithic diatoms to benthic-pelagic coupling in a
763 temperate river. *Aquatic Microbial Ecology* 69, 47–57.

764 Thome, C., Mitz, C., Somers, C.M., Manzon, R.G., Boreham, D.R., Wilson, J.Y., 2016.
765 Incubation of lake whitefish (*Coregonus clupeaformis*) embryos in cooling water
766 discharge and the impacts of fluctuating thermal regimes on development. *Canadian*
767 *journal of fisheries and aquatic sciences* 73, 1213–1221.

768 Traunspurger, W., 1997. Bathymetric, seasonal and vertical distribution of feeding-types of
769 nematodes in an oligotrophic lake. *Vie et Milieu* 47, 1–7.

770 Traunspurger, W., Wilden, B., Majdi, N., 2020. An overview of meiofaunal and nematode
771 distribution patterns in lake ecosystems differing in their trophic state.
772 *Hydrobiologia*, in press; doi: 10.1007/s10750-019-04092-1.

773 Van Vliet, M.T.H., Ludwig, F., Zwolsman, J.J.G., Weedon, G.P., Kabat, P., 2011. Global
774 river temperatures and sensitivity to atmospheric warming and changes in river flow.
775 *Water Resources Research* 47.

776 Vidakovic, J., Palijan, G., Cerba, D., 2011. Relationship between nematode community and
777 biomass and composition of periphyton developing on artificial substrates in
778 floodplain lake. *Polish Journal of Ecology* 59, 577–588.

779 Villanueva, V.D., Font, J., Schwartz, T., Romaní, A.M., 2011. Biofilm formation at warming

780 temperature: acceleration of microbial colonization and microbial interactive effects.
781 Biofouling 27, 59–71.

782 Walker, I.R., Mott, R.J., Smol, J.P., 1996. Allerød-Younger Dryas lake temperatures from
783 midge fossils in Atlantic Canada. Science 253, 1010–1012.

784 Watkinson, A.J., O’Neil, J.M., Dennison, W.C., 2005. Ecophysiology of the marine
785 cyanobacterium, *Lyngbya majuscula* (Oscillatoriaceae) in Moreton Bay, Australia.
786 Harmful Algae 4, 697–715.

787 Webb, B.W., 1996. Trends in stream and river temperature. Hydrological processes 10, 205–
788 226.

789 Weitere, M., Erken, M., Majdi, N., Arndt, H., Norf, H., Reinshagen, M., Traunspurger, W.,
790 Walterscheid, A., Wey, J.K., 2018. The food web perspective on aquatic biofilms.
791 Ecological Monographs 88, 543–559.

792 Weitere, M., Vohmann, A., Schulz, N., Linn, C., Dietrich, D., Arndt, H., 2009. Linking
793 environmental warming to the fitness of the invasive clam *Corbicula fluminea*.
794 Global Change Biology 15, 2838–2851.

795 Woodward, G., Bonada, N., Brown, L.E., Death, R.G., Durance, I., Gray, C., Hladyz, S.,
796 Ledger, M.E., Milner, A.M., Ormerod, S.J., 2016. The effects of climatic
797 fluctuations and extreme events on running water ecosystems. Philosophical
798 Transactions of the Royal Society B 371, 20150274.

799 Woodward, G., Perkins, D.M., Brown, L.E., 2010. Climate change and freshwater
800 ecosystems: impacts across multiple levels of organization. Philosophical
801 Transactions of the Royal Society of London B: Biological Sciences 365, 2093–
802 2106.

803 Worthington, T.A., Shaw, P.J., Daffern, J.R., Langford, T.E.L., 2015. The effects of a
804 thermal discharge on the macroinvertebrate community of a large British river:

805 implications for climate change. *Hydrobiologia* 753, 81–95.

806 Yvon-Durocher, G., Montoya, J.M., Trimmer, M., Woodward, G., 2011. Warming alters the

807 size spectrum and shifts the distribution of biomass in freshwater ecosystems. *Global*

808 *Change Biology* 17, 1681–1694.

809 **Tables**

810 **Table 1.** Mean, standard deviation (SD), and minimum (Min) and maximum (Max) values of
 811 the variables measured or indices computed at each site (N = 20 samples for each site).
 812 Differences were tested using one-way ANOVA or Kruskal-Wallis rank sum test depending
 813 on whether the data met the linear assumptions or not, respectively. The level of significance
 814 (p-values: * = 0.01–0.05; ** = 0.001–0.01; *** < 0.001) is given. Full test statistics are
 815 provided in Table S3. Mean values highlighted in bold show significantly higher values at a
 816 given site.
 817

Variables	Control site				Heated site				Test signif.
	Mean	SD	Min	Max	Mean	SD	Min	Max	
Pigment concentrations (ng.mgBiofilmDM ⁻¹)									
Chlorophyll <i>a</i>	254.49	42.41	21.51	713.53	240.71	23.21	66.59	418.75	
Fucoxanthin	83.72	13.10	4.49	221.34	71.59	8.95	21.78	154.10	
Chlorophyll <i>b</i>	25.15	5.51	1.77	119.52	7.36	1.11	1.11	18.40	***
Diadinoxanthin	13.05	2.31	1.31	39.67	10.19	1.46	2.35	24.22	
Chlorophyllide <i>a</i>	10.48	7.58	0.00	156.57	46.15	14.45	0.00	190.65	**
Hexanoyloxy fucoxanthin	8.44	1.45	0.00	18.65	10.99	1.28	0.29	21.91	
Zeaxanthin	7.66	1.48	0.46	25.06	13.48	1.48	3.06	24.42	*
Violaxanthin	5.78	1.24	0.45	26.40	2.27	0.20	1.01	4.61	*
Lutein	5.67	1.03	0.00	19.23	1.98	0.26	0.00	4.35	**
Pheophytin <i>a</i>	4.79	0.79	0.00	13.81	6.26	0.64	0.00	13.09	
Alloxanthin	1.82	0.38	0.00	5.38	2.05	0.36	0.00	5.36	
β Carotene	0.99	0.14	0.00	2.57	1.64	0.18	0.57	3.14	**
Myxoxanthophyll	0.81	0.58	0.00	10.99	1.80	0.32	0.00	4.49	***
Echinenone	0.00	0.00	0.00	0.00	0.89	0.25	0.00	3.80	***
Abundance (ind.10cm ⁻²)									
Total invertebrates	335.22	38.30	157.17	839.54	295.87	17.34	145.23	467.52	
Nematodes	91.12	8.66	37.80	194.96	139.98	11.80	27.85	228.79	**
Rotifers	85.05	6.09	27.85	137.27	94.30	7.86	41.78	185.02	
Chironomids	60.38	6.31	1.99	123.35	39.81	4.92	6.37	97.48	*
<i>Corbicula</i>	55.80	16.82	0.00	326.27	3.76	1.16	0.00	17.90	***
Harpacticoids	19.70	6.09	0.00	109.42	3.68	1.00	0.00	17.90	**
Nauplii	8.06	2.14	0.00	33.82	2.19	0.54	0.00	9.95	*
Oligochaetes	7.56	2.36	0.00	33.82	9.67	1.34	0.00	21.88	*

Ephemeroptera	5.67	1.04	0.00	17.90	1.39	0.45	0.00	7.96	***
Ostracods	1.59	0.41	0.00	5.97	0.90	0.36	0.00	5.97	
Cladocers	0.30	0.16	0.00	1.99	0.20	0.13	0.00	1.99	
Biomass ($\mu\text{gDM} \cdot 10\text{cm}^{-2}$)									
Total invertebrates	385.75	51.43	43.17	996.37	284.54	58.11	12.01	1080.08	
Chironomids	227.82	31.61	0.28	472.95	247.14	56.17	3.14	1041.08	
Ephemeroptera	79.59	16.98	0.00	294.06	16.97	5.67	0.00	92.53	***
Harpacticoids	48.19	17.02	0.00	345.32	5.69	1.94	0.00	33.99	***
<i>Corbicula</i>	13.57	4.09	0.00	79.36	0.91	0.28	0.00	4.35	***
Oligochaets	6.83	2.65	0.00	40.73	6.27	1.07	0.00	21.46	
Ostracods	5.23	1.36	0.00	19.62	2.94	1.18	0.00	19.62	*
Nauplii	3.06	0.82	0.00	12.67	0.82	0.20	0.00	3.73	*
Nematodes	0.94	0.11	0.21	2.20	3.28	0.38	0.36	7.16	***
Rotifers	0.41	0.03	0.13	0.63	0.45	0.04	0.19	0.85	
Cladocers	0.10	0.05	0.00	0.64	0.06	0.04	0.00	0.64	
Nematode feeding types (%)									
Deposit-feeders	84.23	2.35	54.55	100.00	54.19	2.49	28.21	75.00	***
Epistrate-feeders	12.81	2.50	0.00	45.45	33.12	2.78	10.00	61.54	***
Chewers	1.91	0.83	0.00	15.38	6.79	1.14	0.00	18.75	***
Suction-feeders	0.92	0.43	0.00	6.25	5.90	0.97	0.00	12.50	***
Nematode diversity indices									
Species richness (S)	4.40	0.24	3.00	7.00	6.95	0.32	5.00	10.00	***
Shannon's entropy (H)	1.09	0.04	0.73	1.45	1.48	0.05	0.94	1.90	***
Simpson's dominance (D)	0.40	0.02	0.27	0.61	0.30	0.02	0.19	0.54	***
Pielou's evenness (J)	0.76	0.03	0.53	0.96	0.77	0.02	0.59	0.92	
Trophic diversity (ITD)	0.75	0.03	0.50	1.00	0.44	0.02	0.30	0.59	***

818

819

820

821

822

823

824

825

826

827

828

829 **Table 2.** Mean (ind 10cm⁻²) and relative (%) abundance of biofilm-dwelling nematode
830 species. Abbreviations for nematode species names are provided in Table S5. Suffixes refer
831 to species feeding types (DF = deposit-feeders; EF = epistrate-feeders; C = chewers; SF =
832 suction-feeders).

833

Control site			Heated site		
Species	Mean (ind.10cm ⁻²)	%	Species	Mean (ind.10cm ⁻²)	%
MonParaDF	38.06	41.77	EuVulgDF	46.89	33.50
EuVulgDF	37.90	41.59	ChroBiocEF	45.86	32.76
ChroBiocEF	7.84	8.61	MonParaDF	18.95	13.54
MonPaluDF	1.92	2.10	MyloLacC	8.80	6.29
EuSimpDF	1.66	1.82	DoryBasSF	7.20	5.14
TobStefC	1.10	1.21	EuSimpDF	2.49	1.78
DoryStagSF	1.03	1.13	RhabAquaDF	2.00	1.43
IroTenuC	0.42	0.46	EuDispDF	1.71	1.22
EuPseuDF	0.38	0.42	EuPseuDF	1.52	1.08
EthmoPratEF	0.27	0.30	RhabTerrDF	1.25	0.90
TripGloC	0.15	0.16	TobStefC	1.16	0.83
EuDispDF	0.13	0.15	DoryStagSF	0.68	0.49
Mermi-Par	0.13	0.15	MonPaluDF	0.54	0.39
PlecAquaDF	0.13	0.14	PlecAquaDF	0.36	0.26
			EuLongDF	0.24	0.17
			ChroVirEF	0.20	0.15
			DoryAgiSF	0.14	0.10

834

835

836

837

838

839

840

841 **Figure caption**

842 **Fig. 1.** Aerial view of the study site (source: IGN 2020) and photographs of the experimental
843 set-up at the heated and control sites.

844

845 **Fig. 2. A.** Hourly water temperature recorded at the control (green line) and heated (orange
846 line) sites over the entire experimental period (1344 h, starting on 7 August 2018 at 1 PM and
847 ending when the samples were retrieved on 2 October 2018 at 1 PM). **B.** Boxplots of the
848 daily fluctuation of water temperature (i.e., the range between the minimum and maximum
849 water temperature for each day) at each site over the entire period. **C.** Hourly ΔT (difference
850 in water temperature between heated and control sites).

851

852 **Fig. 3.** Non-metric multidimensional scaling (nMDS) of the Bray–Curtis similarities of
853 pigment composition across samples (N = 40 concrete tiles). Pigment concentrations are
854 ordinated on the biplot. ‘spider web’ extremities indicate the position of the samples in the
855 2D-space. The labels in black (control or heated) indicate the centroid of the site they belong
856 to, and the labels in red indicate the centroid of each pigment concentration (pigment
857 abbreviations can be found in Table S5).

858

859 **Fig. 4.** Non-metric multidimensional scaling (nMDS) of the Bray–Curtis similarities of
860 invertebrate group abundances across samples. Group abundances are ordinated on the biplot.
861 ‘spider web’ extremities indicate the position of the samples in the 2D-space. The label in
862 black (control or heated) indicate the centroid of the site they belong and the labels in red
863 indicate the centroid of each invertebrate group (group abbreviations can be found in Table
864 S5).

865

866 **Fig. 5. A.** Chironomid body-mass distribution at each site (heated site: dark orange, control
867 site: green). Vertical dotted lines indicate the mean body-mass value for each site. **B.**
868 Cumulative density functions for chironomid individual body-mass.

869

870 **Fig. 6.** Non-metric multidimensional scaling (nMDS) of the Bray–Curtis similarities of
871 nematode species abundances across samples. Species abundances are ordinated on the
872 biplot. ‘spider web’ extremities indicate the position of the samples in the 2D-space. The
873 label in black (control or heated) indicate the centroid of the site they belong and the labels in
874 red indicate the centroid of each species (species abbreviations can be found in Table S5;
875 suffixes refer to species feeding type, see Table 2).

876

877 **Fig. 7.** Relative abundance of nematode feeding types across sites. Values are medians, boxes
878 and whiskers show interquartile range.

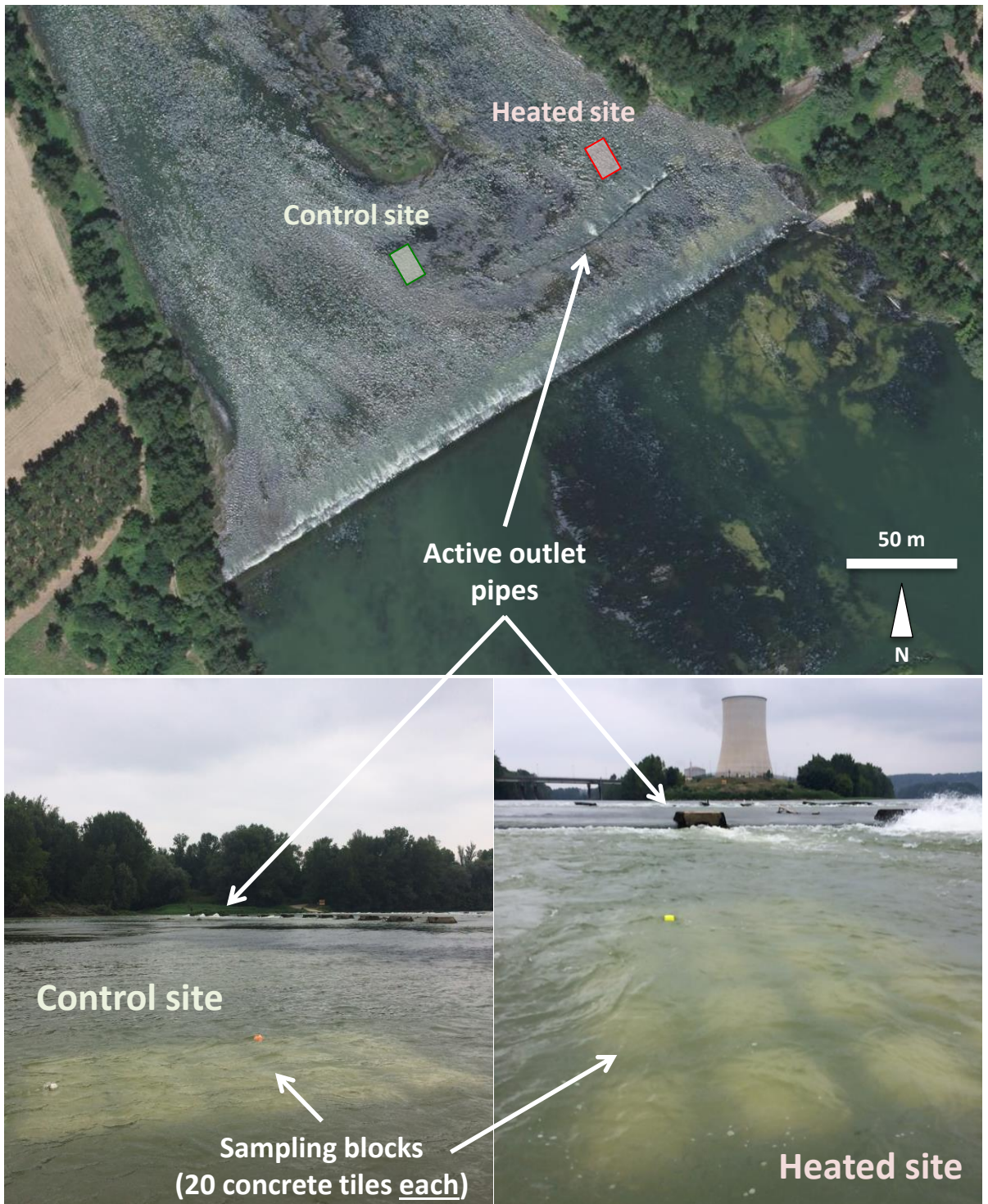


Fig. 1

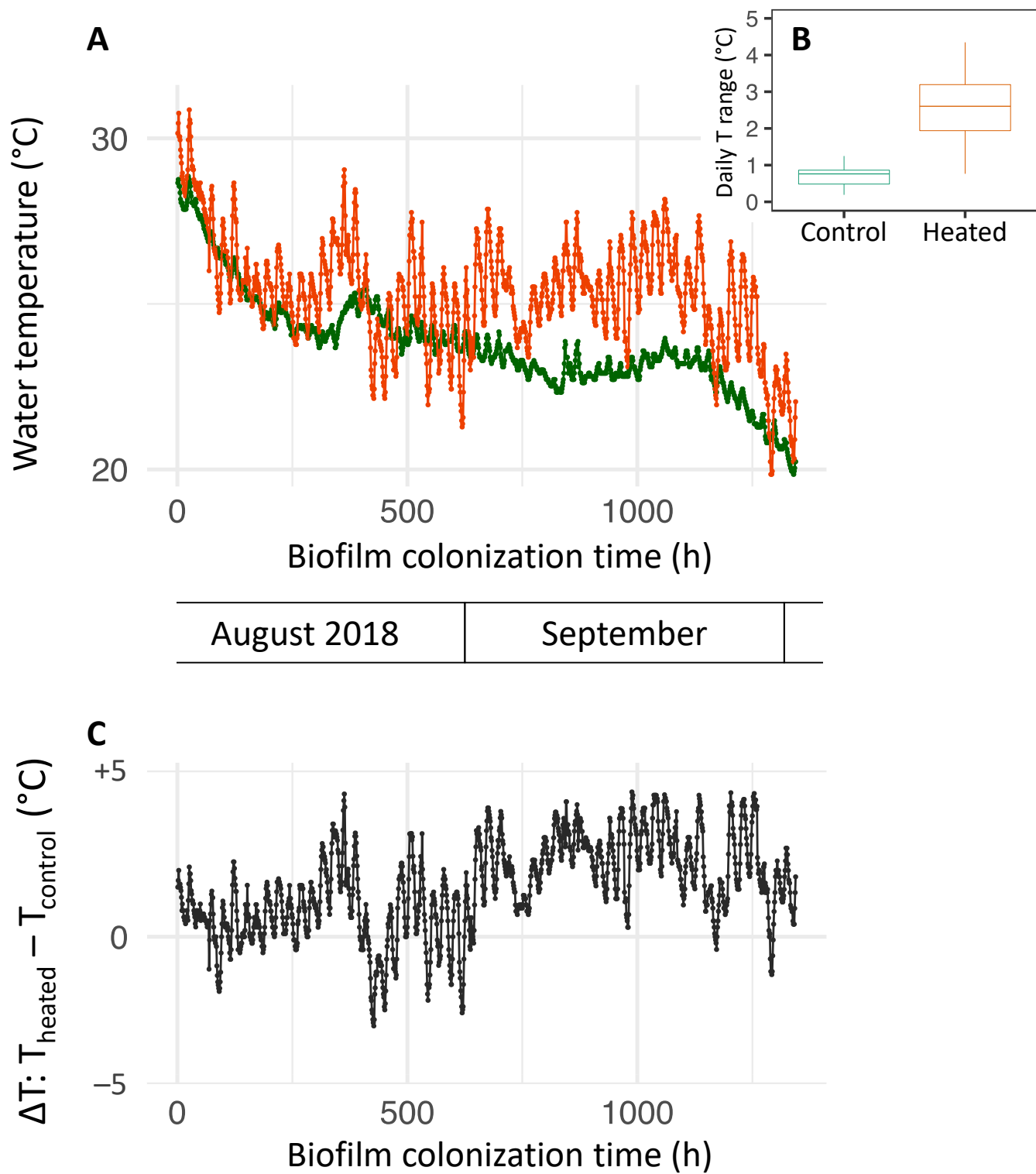


Fig. 2

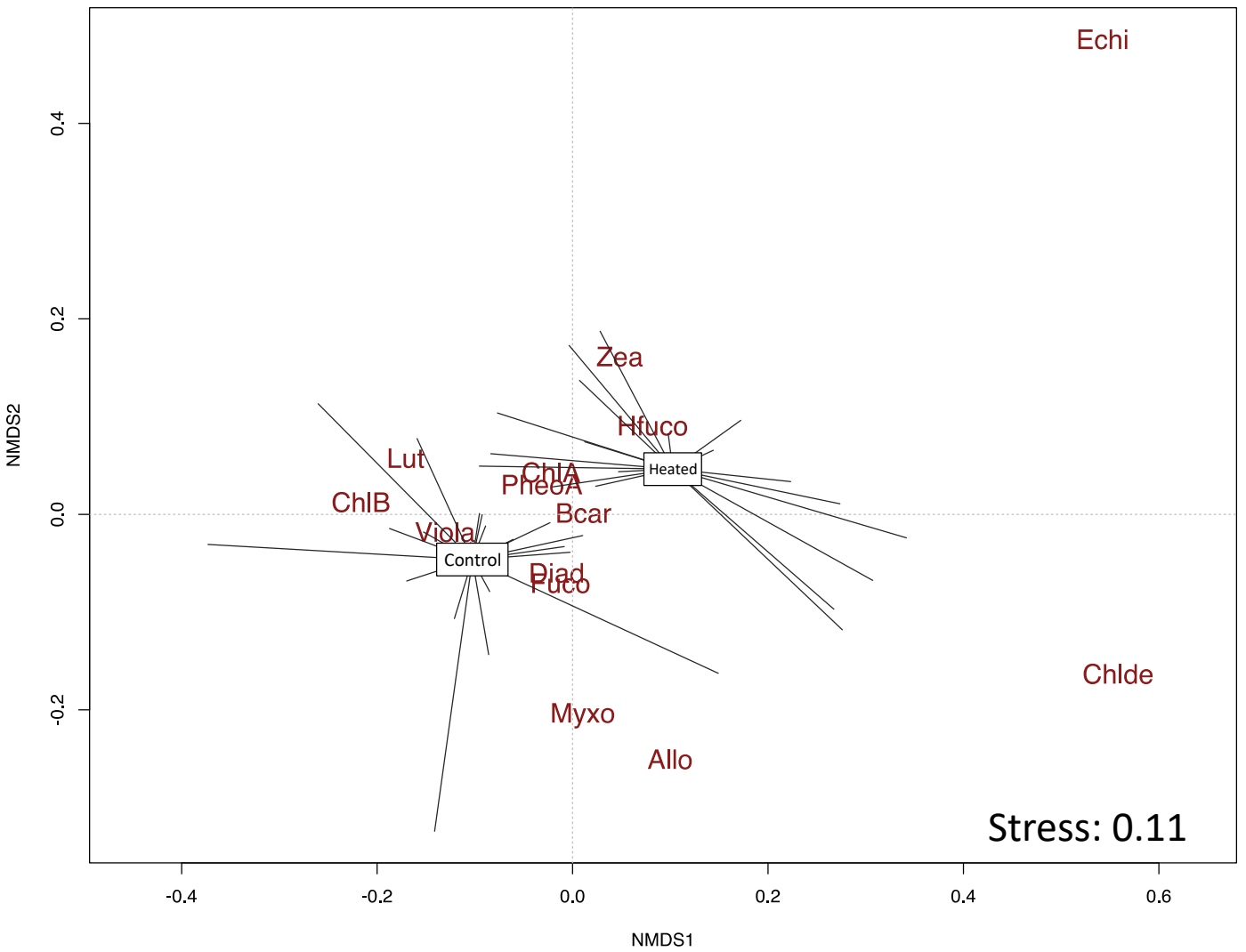


Fig. 3

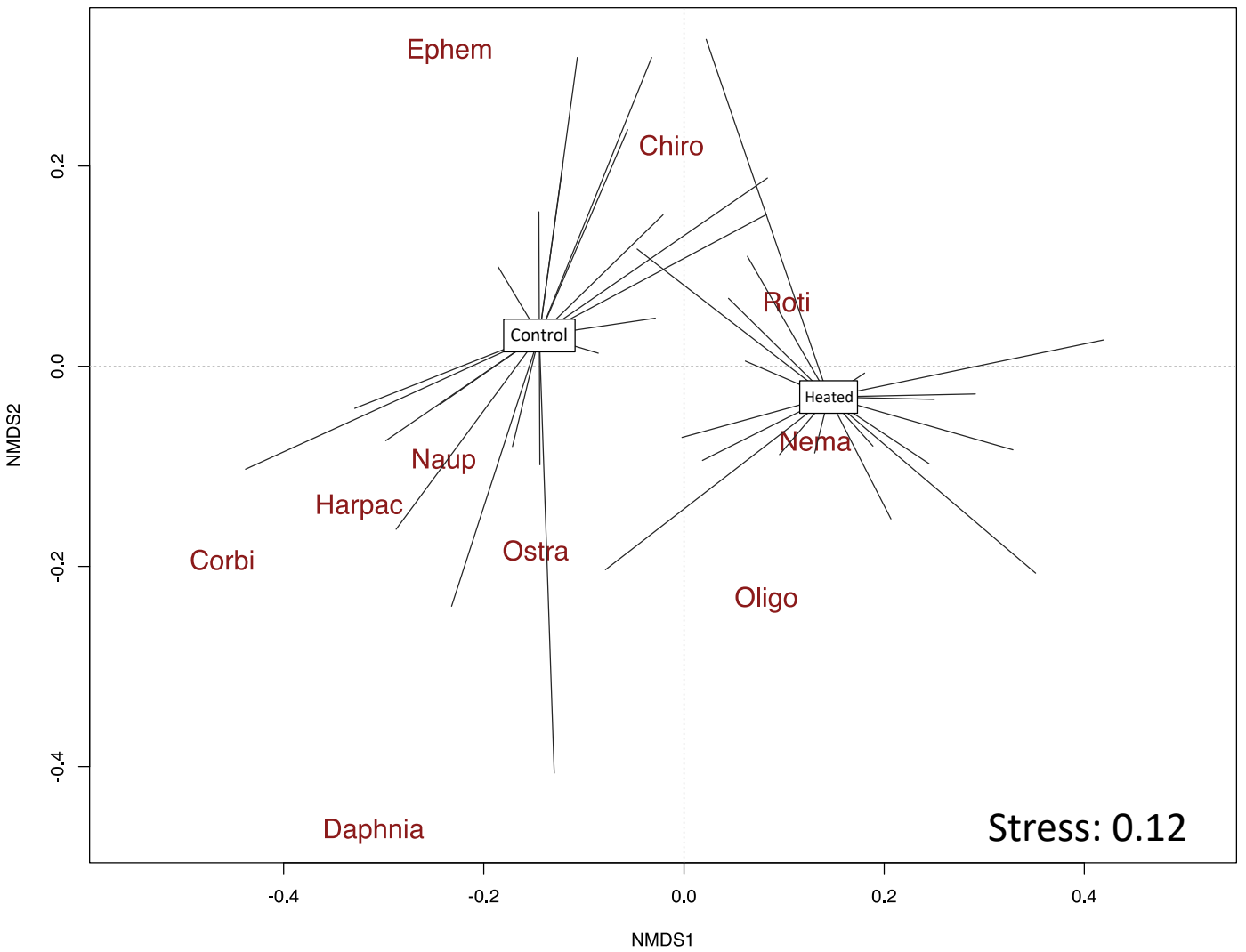
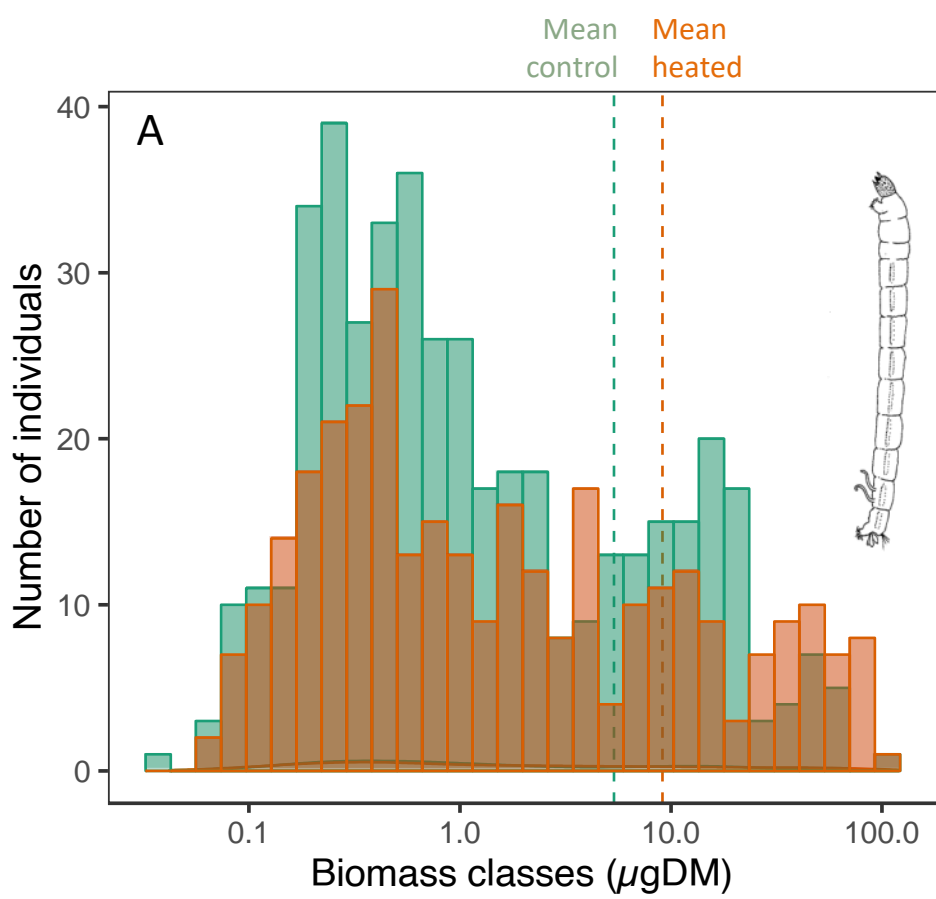


Fig. 4



Cumulative body-mass distribution of chironomids

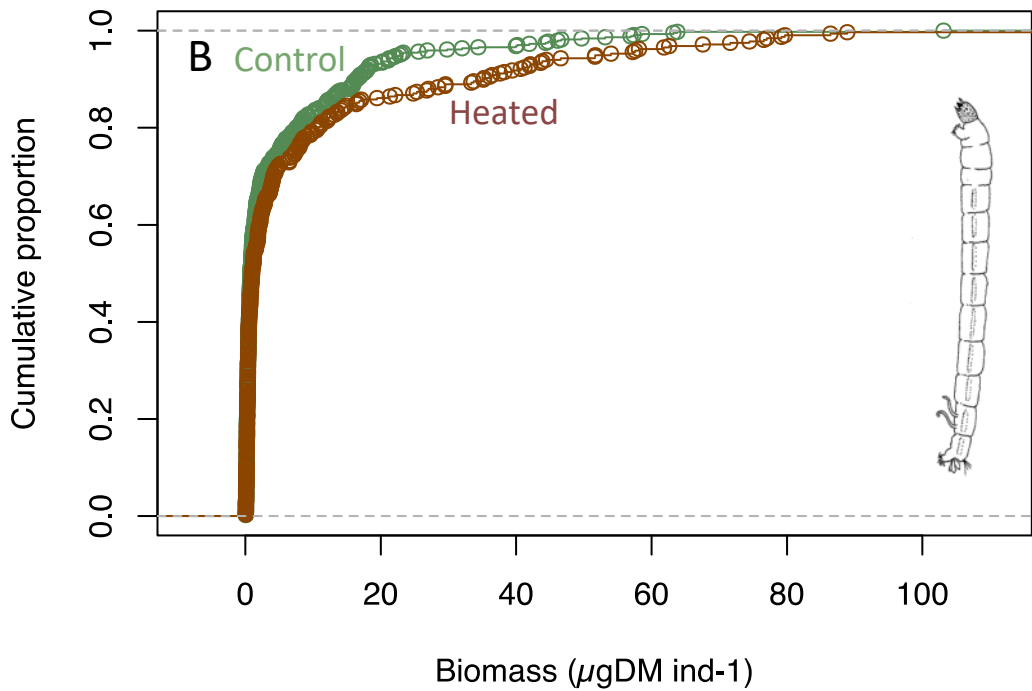


Fig. 5

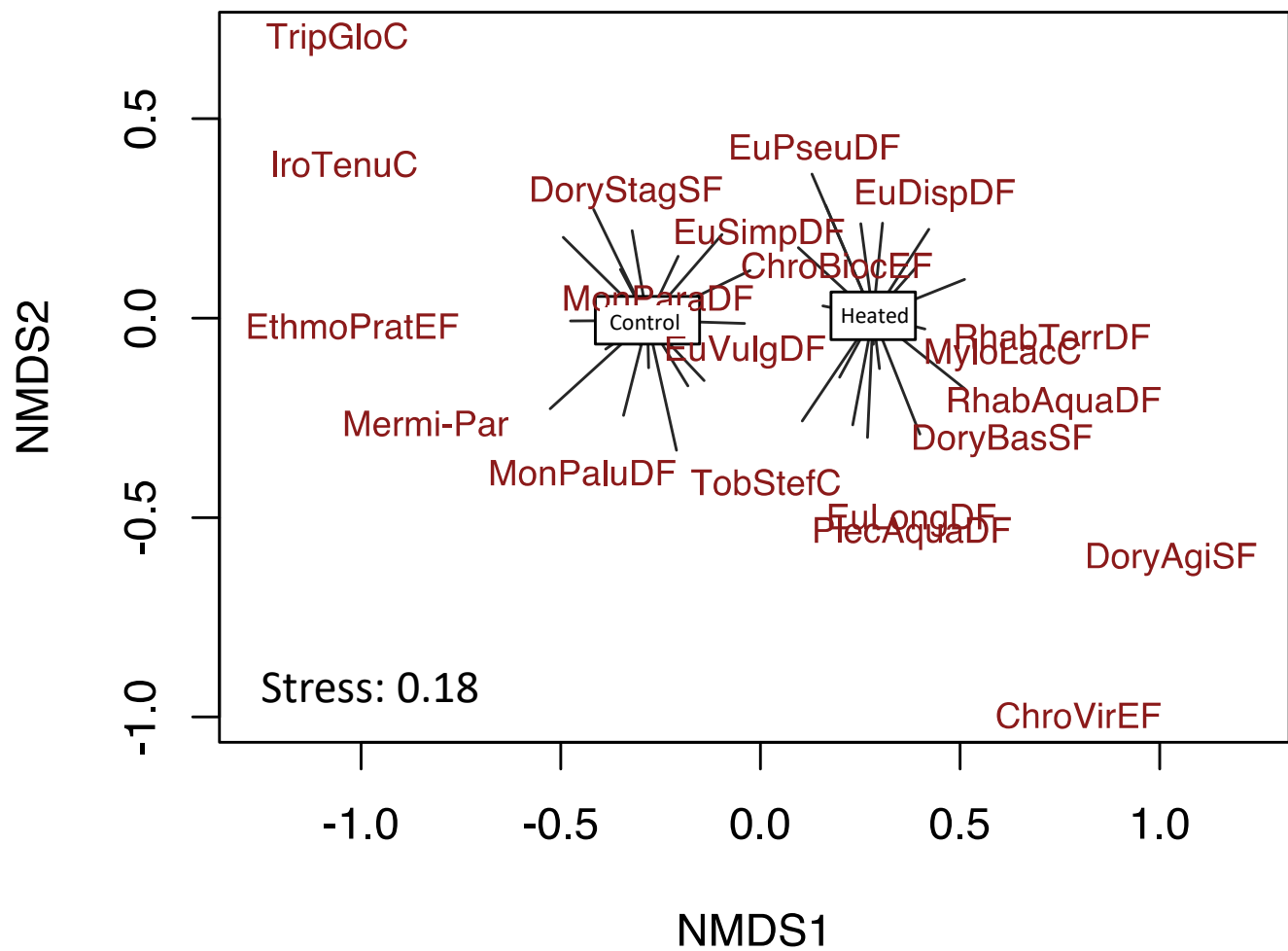


Fig. 6

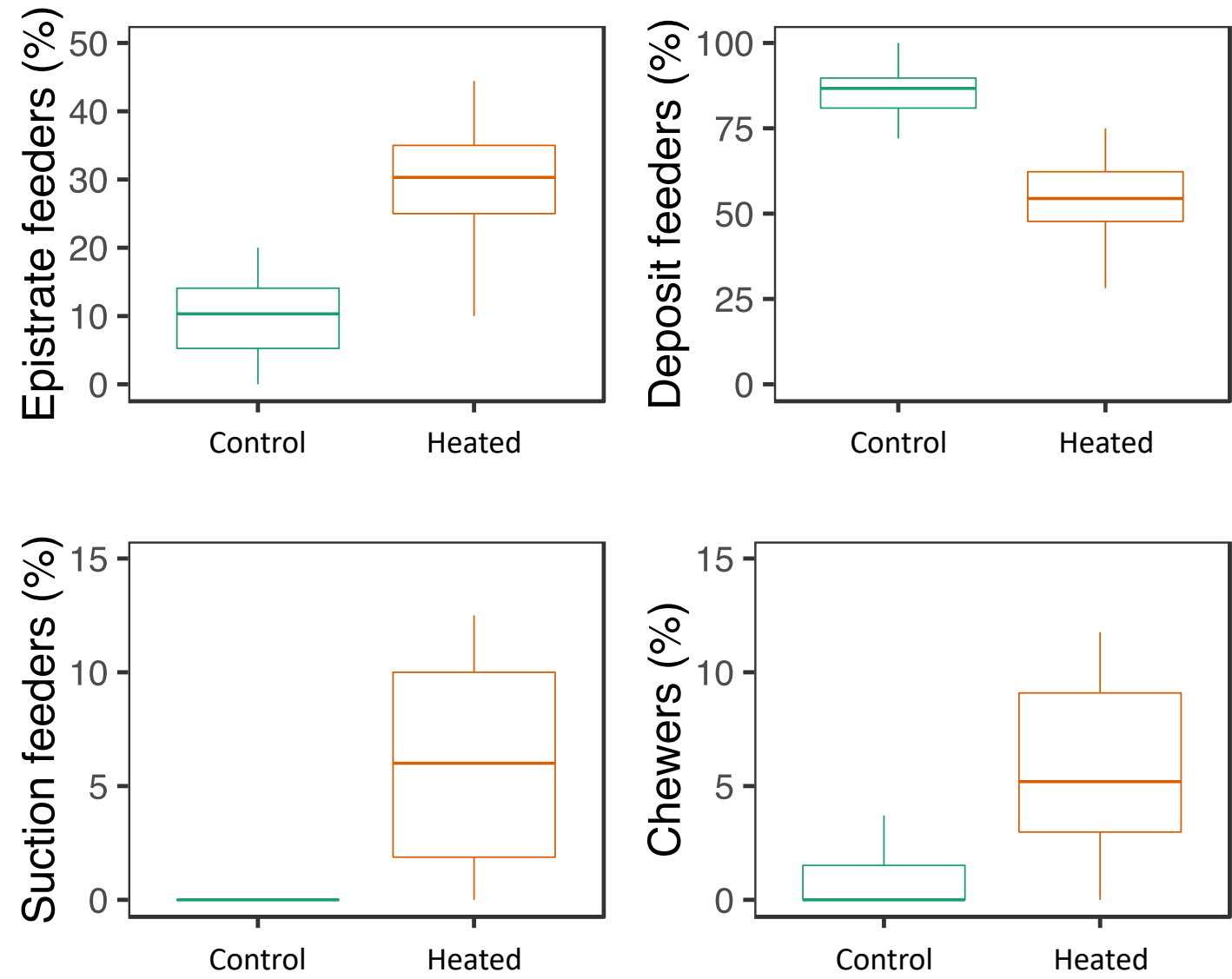


Fig. 7

In situ warming experiment in the Garonne River (France)

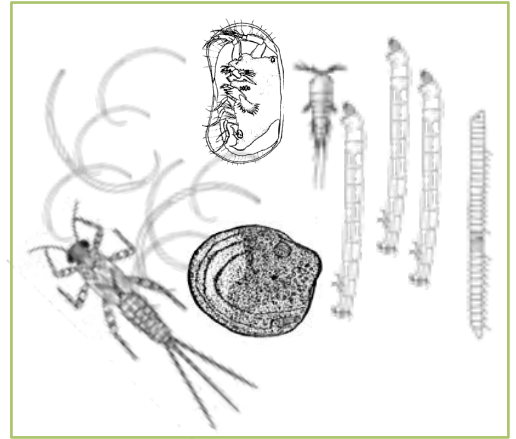
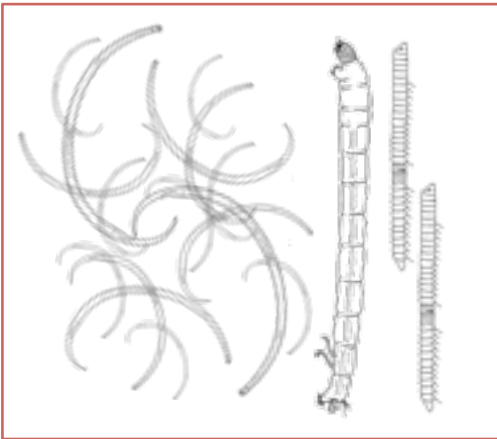
Heated site



Control site



Biofilm-dwelling communities



**Comparable standing stocks
Different assemblages**